Evaluation of seismic reliability and multi level response reduction factor (R factor) for eccentric braced frames with vertical links

Vahid Mohsenian[a] and Alireza Mortezaei[*]

Seismic Geotechnical and High Performance Concrete Research Centre, Civil Engineering Department,
Semnan Branch, Islamic Azad University, Semnan, Iran

Abstract. Using vertical links in eccentric braced frames is one of the best passive structural control approaches due to its effectiveness and practicality advantages. However, in spite of the subject importance there are limited studies which evaluate the seismic reliability and response reduction factor (R-factor) in this system. Therefore, the present study has been conducted to improve the current understanding about failure mechanism in the structural systems equipped with vertical links. For this purpose, following definition of demand and capacity response reduction factors, these parameters are computed for three different buildings (4, 8 and 12 stories) equipped with this system. In this regards, pushover and incremental dynamic analysis have been employed, and seismic reliability as well as multi-level response reduction factor according to the seismic demand and capacity of the frames have been derived. Based on the results, this system demonstrates high ductility and seismic energy dissipation capacity, and using the response reduction factor as high as 8 also provides acceptable reliability for the frame in the moderate and high earthquake intensities. This system can be used in original buildings as lateral load resisting system in addition to seismic rehabilitation of the existing buildings.

Keywords: vertical links; eccentric braced frame; response reduction factor; seismic reliability

1. Introduction

Eccentric brace system with vertical links is one of the passive structural control systems, which can provide both stiffness and ductility for the building structures. Due to its simple mechanism, replaceability and easy design and construction, this system is applicable not only for design of new structures, but also for rehabilitation of existing buildings. This system was proposed by Seki *et al.* (1988) as a lateral load bearing system. They reported that hysteresis curves of the system are stable and symmetric. Daryan *et al.* (2008) investigates the effects of using mild steel instead of conventional structural steel for the shear panels (vertical links). They found that in contrast to the shear panels with structural steel, using mild steel cause no local buckling occurs in the vertical links. Furthermore, employing mild steel would increase seismic energy dissipation and ductility considerably, which in turns improves seismic performance of the frame structure. Lian and Su (2017) evaluated experimentally and numerically the response reduction factor for two different frame components of the eccentric braced system with vertical links. The results of frames with high strength steel demonstrate desirable cyclic behavior (stable hysteresis loops without stiffness degradation), high seismic energy dissipation and load bearing capacity.

Rahnavard *et al.* (2017) studied the effects of double and single vertical links on the seismic behavior of eccentric braced frames. Relying on their findings, using double instead of the single vertical links results in more stable hysteresis curves which increases seismic energy dissipation and shear capacity of the frames considerably. They also observed an improvement in the frame seismic behavior due to increase in the link spacing.

Duan and Su (2017) did some experimental tests on the braced frame structures equipped with vertical dampers having different lengths. They were focused mainly on the nonlinear deformations of the vertical links. It was observed that in a given displacement, the vertical links with shear performance demonstrate more ductility and energy dissipation capacity in comparison to those with the bending behavior. According to the analytical and experimental studies, some design relationships were proposed for the braced frame structures with vertical links by Vetr *et al.* (2017), Bouwkamp *et al.* (2016). They reported that the maximum shear strength of the link is 2.2 times of its nominal strength and the P-Delta effects are negligible.

Baradaran *et al.* (2015) concluded that the frame structures equipped with the vertical links demonstrate desirable behavior and possess stable hysteresis curves. According to their findings, beams with the punched webs which are strengthened by the shear plates do not experience any negative effect on their hysteresis curves.

Analytical studies by Zahrai and Parsa (2015) evaluated the effects of flange width on the cyclic behavior of frame system. Based on the results, when the vertical link has enough support, any reduction in the flange width has no

---

∗Corresponding author, Associate Professor
 E-mail: a.mortezaei@semnaniau.ac.ir
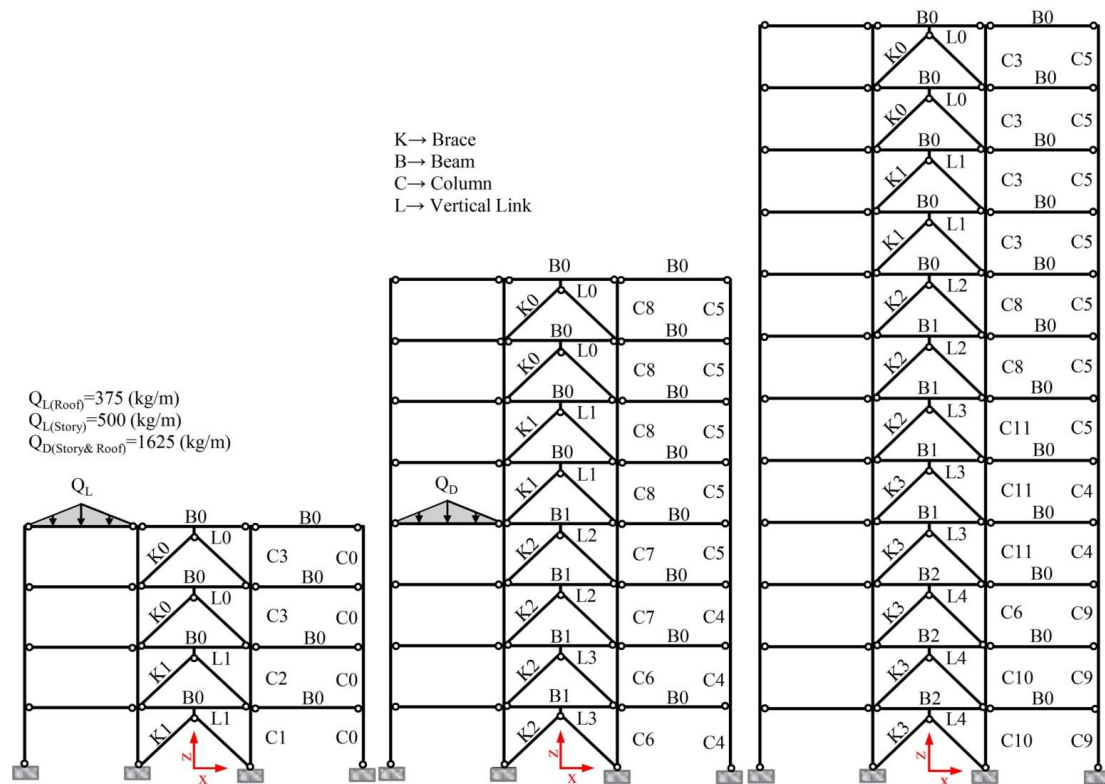[a]Senior Researcher

Fig. 1 Geometrical properties of the studied frame structures and details of the gravitational loading

negative effect on hysteresis curves and energy dissipation capacity. Another study by Zahrai and MoslehiTabar (2013) showed that damping ratio and plastic rotation of the links in a frame equipped with shear links equal to 30 percent and 0.15 radian, respectively.

Shayanfar *et al.* (2011) evaluated the effects of stiffeners on the web of shear links and found that using stiffeners result in promoting the shear capacity and ductility of the links.

Zahrai and Mahroozadeh (2010) estimated the response reduction factor of frames equipped with the shear link between 7.15 and 10.65.

Reviewing past studies show that there are limited analytical and experimental studies regarding seismic reliability and response reduction factor for eccentric braced systems equipped with the shear links, especially in multi-story structures. Therefore, the present study uses a different approach to estimate the response reduction factor (R-factor) of this system based on the intensity of applied excitation and the allowable damage level in the range of nonlinear behavior. For this purpose, push-over and incremental dynamic analyses (IDA) are utilized.

2. Methodology

2.1 Properties of the studied frames

In this study, 4, 8 and 12 story frames with the geometrical properties and live (Q_L) and dead (Q_D) loads depicted in Fig. 1 are used. The structure belongs to a residential building category which is located in the area

Table 1 Properties of sections used for structural members

Symbol	Section	Symbol	Section	Symbol	Section	Symbol	Section
C0	2IPE12	C6	BOX (40×40×2.5)	K0	2UNP10	B2	IPE36
C1	BOX (30×30×2.0)	C7	BOX (35×35×1.5)	K1	2UNP12	L0	IPE16
C2	BOX (25×25×1.0)	C8	BOX (30×30×0.8)	K2	2UNP14	L1	IPE20
C3	BOX (25×25×0.5)	C9	2IPE18	K3	2UNP16	L2	IPE24
C4	2IPE16	C10	BOX (45×45×2.5)	B0	IPE24	L3	IPE27
C5	2IPE14	C11	BOX (35×35×1.0)	B1	IPE30	L4	IPE30

with high seismicity. Story height is equal to 3.2 meters and each span is 5 meters wide. The site soil is type II (375 m/s≤V_s≤750 m/s) according to the Iranian Code of Practice for Seismic Resistant Design of Buildings (Standard No. 2800, 2014).

The frame structures are designed according to the Iranian National Building Code for steel structures design Part 10 (2008) using the ETABS software (CSI-2015). The response reduction factor used for the preliminary design is taken equal to 7 relying on the Iranian Code of Practice for Seismic Resistant Design of Buildings (Standard No. 2800, 2014) for the special eccentric braced systems. Base shear coefficients of 4-, 8- and 12-story frames are determined 0.125, 0.115 and 0.105, respectively. It must be noted that all of the structural components in the braced spans, namely braces, beams and columns, are controlled for the intensified earthquake (Ω_0=2). In Iranian Code of Practice for Seismic Resistant Design of Buildings (Standard No.

2800, 2014) an intensified earthquake is achieved by applying Ω_0 coefficient on the design hazard level. All force-control parameters, which have the probability of brittle failure, are controlled under the intensified earthquake.

Effects of rigid diaphragm and nodes coupling at the story level are also included in the model. Properties of the structural members (beams, columns and braces) are depicted in Fig. 1 and listed in Table 1. Moreover, as shown in Fig. 1, the frame is symmetric with respect to the *z* axis.

2.2 Nonlinear modeling and evaluation of strength and deformation parameters

To analyze the structures in the range of nonlinear behavior, PERFORM-3D software (CSI-2016) is used. As all beam and column connections of the frame are assumed to be hinged, therefore is not expected that these members in the side spans enter the nonlinear range. Therefore, beams and columns are modeled by using the standard sections, assuming that their behavior is linear.

To control the failure mechanism and catch better insight about the energy dissipation of different structural elements, in addition to the vertical link, story beams and braces are also modeled as nonlinear elements.

2.2.1 Brace element modeling

Modeling and control of acceptance criteria for braces in the nonlinear range is done based on the generalized load-displacement relationship which is shown in Fig. 2. The parameters which are used to define ductility and nonlinear behavior of structural members depends on the type of members. For braces with hinge connections which dissipate energy by means of axial forces, the selected parameters are axial deformations at the expected buckling load, (Δ_c) and at the tensile yield force (Δ_t) (FEMA 356 2000).

Assuming clear length equal to *L*, to compute the axial deformations, (Δ), from the relation presented in Fig. 2, expected strength of the brace members, (T_{CE}), and the lower bound of the strength under the compression force, (P_{CL}), are used as the member force, (*F*). The other parameters namely *a*, *b* and *c* are derived from the modeling tables and the acceptance criteria of nonlinear methods, based on the failure mode and properties of the brace section, which is double-channel in this study (FEMA 356 2000).
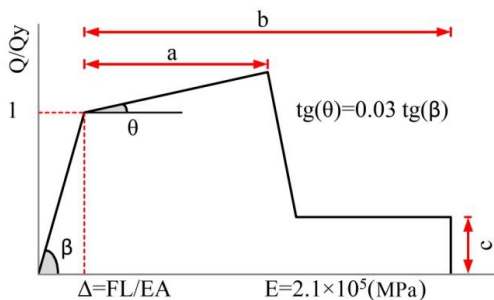
In the software, bar elements, which only can bear axial force, are used to model the braces. According to Fig. 3, after analyzing the eccentric braced frame with vertical links it is demonstrated that following shear yielding of the vertical link, the axial forces in the braces (*F*) and therefore the tensile and compressive displacements in the elements (Δ_1&Δ_2) and root of their squares (Δ') remains constant. Consequently, in the higher intensity of ground motions, increase in the shear strains of the links only leads to the increase in the story lateral displacement (Δ_S). It is necessary to consider this behavior when designing the brace elements.

To model the braces in the software, "steel bar/tie/strut" elements are used which only resists axial forces.

2.2.2 Beam modeling in the braced spans

Based on the free body diagram of story beams, which is shown in Fig. 4, and using the equilibrium equations, it is resulted that the shear forces along the beam is constant. In addition, due to concentrated moment of the vertical link connection (*M*), the maximum bending moment occurs in the middle of beam. Accordingly, the linear "beam" elements with "shear-plastic strain type" and "moment-rotational type" hinges in their mid-span are used to model story beams.

It is noteworthy to mention that the flexural and shear capacity of the sections are estimated equal to ZF_{ye} and
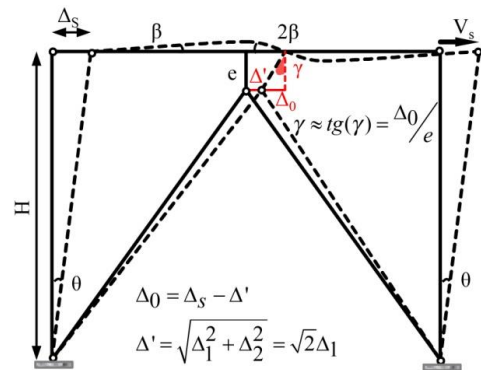

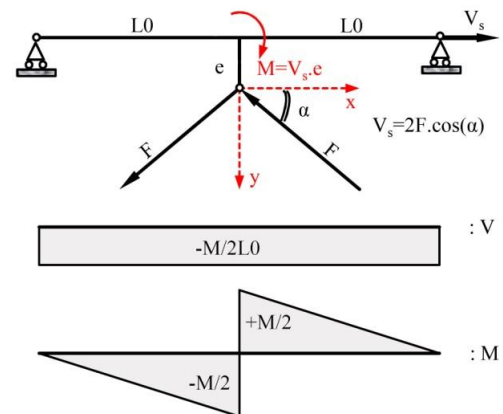Fig. 3 Schematic displacements of the frame members under lateral loading

Fig. 4 Free diagram of the story beam and variation of the shear force and bending moments in the beam

Fig. 2 Generalized load-displacement curve for steel sections

0.55$F_{ye}.Aw$, respectively. In thgese relations, Z and A_w are plastic section modulus and web cross section area (without considering flanges), F_{ye} is the expected yield stress of steel.

2.2.3 Modeling vertical links

The vertical links are designed such that they yield before the other elements of frame and therefore act like seismic fuse in the design hazard level.

To achieve desirable performance of shear yielding, the length of the links, e, is selected equal to 20 cm (Bathaei and Zahrai 2017). After computing the shear and bending capacity of elements (V_{CE}&M_{CE}), the link length equal to 20 cm is compared with the $1.6M_{CE}/V_{CE}$ ratio. Evaluations shows that the links will surely have shear behavior ($e \leq (1.6M_{CE}/V_{CE})$). Thus, performance of the links is based on the expected shear strength of the beam (V_{CE}).

The link sections are designed according to the before description. Then, capacity and deformation angle of the link (γ), based on the actual loading conditions (interaction of shear forces and bending moments) are computed by using the ABAQUS (2014) and the corresponding curves are also extracted. The resulted capacity curve is idealized by an equivalent bilinear curve in order to be used in the PERFORM-3D software.

It is necessary to mention that the shear capacity of the section is relatively close to the value derived from the equation 0.55$F_{ye}.Aw$.

Shear deformation angle of the link (γ) is another important factor in the design. In many standards and codes, this parameter is limited to 0.08 and 0.09for the shear deformable elements (Bathaei and Zahrai 2017). In the present study, shear deformation angle of the vertical links is limited to the mentioned values. After extraction and adjustment of the capacity-deformation curves, as shown in Fig. 5, four different failure modes based on the maximum stresses is defined.

To model vertical links in the software, linear "column" elements with concentrated "shear-plastic strain type" hinges are used. It is evident in the Fig. 5 that the stress level in the flanges are always less than web. This verifies nonlinear modeling and assumption of the shear yielding in the web of vertical links.

3. Nonlinear static and dynamic analysis

In the developed model, values of the applied dead and live loads are same as the initial design step. For combination of the lateral and gravitational loads, the upper limit of gravitational loads is considered as Eq. (1) (FEMA 356 2000)

$$Q_G = 1.1[Q_D + Q_L] \tag{1}$$

Where Q_D and Q_L are dead and live loads, respectively.

3.1 Eigen value analysis

Vibrational periods and coefficients of the frame effective translational mass participation are computed for the first four modes and the results are listed in Table 2.
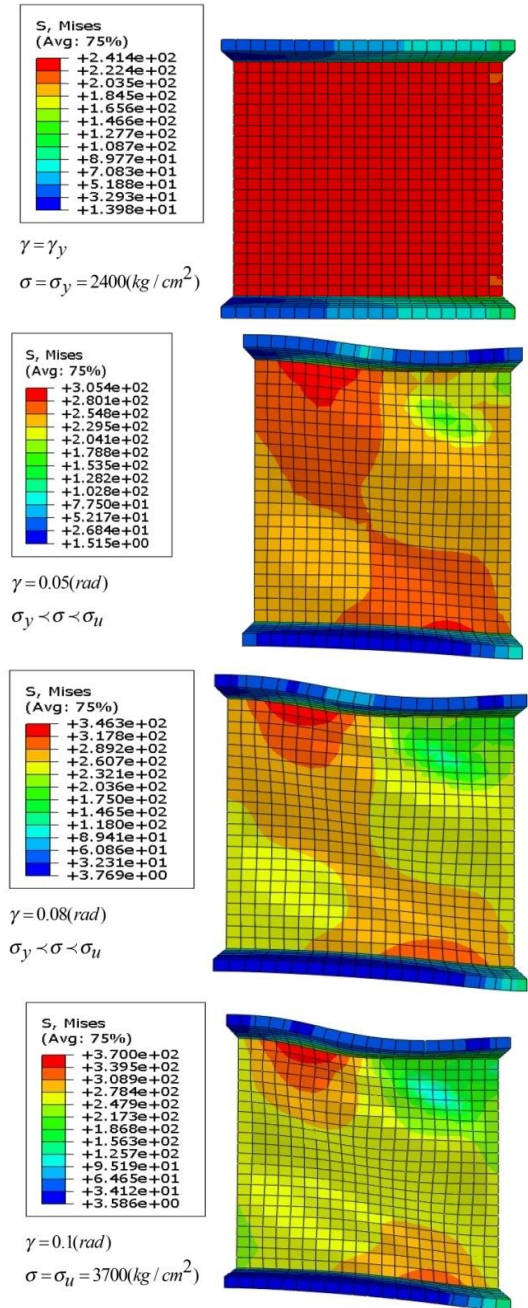

$\gamma = \gamma_y$

$\sigma = \sigma_y = 2400(kg/cm^2)$

$\gamma = 0.05(rad)$

$\sigma_y \prec \sigma \prec \sigma_u$

$\gamma = 0.08(rad)$

$\sigma_y \prec \sigma \prec \sigma_u$

$\gamma = 0.1(rad)$

$\sigma = \sigma_u = 3700(kg/cm^2)$

Fig. 5 Sample of deformations and maximum stresses in the links

Table 2 Vibrational periods (T) and coefficients of effective translational mass participation (M)

Mode Number	4 story frame		8 story frame		12 story frame	
	T (Sec)	M (%)	T (Sec)	M (%)	T (Sec)	M (%)
1	0.175	83.70	0.339	73.0	0.646	63.5
2	0.065	12.98	0.121	18.8	0.204	24.1
3	0.038	2.36	0.066	4.47	0.106	6.70
4	0.028	0.95	0.045	1.78	0.07	2.37

The fundamental periods of vibration of the 4, 8 and 12 story frame structures with eccentric braced frames are 0.54, 0.91 and 1.24 seconds by means of Eq. (2) which is recommended by Iranian Code of Practice for Seismic

Table 3 Maximum drift in the design earthquake (%)

4 story frame	8 story frame	12 story frame
0.0652	0.136	0.245

Table 4 The ground motions used to produce artificial accelerograms and doing incremental dynamic analysis

Record Number	Earthquake & Year	Station	R^a (km)	Component	Ms	PGA (g)
R1	Cape Mendocino, 1992	Eureka - Myrtle & West	41.97	90	7.1	0.1782
R2	Northridge, 1994	Hollywood – Willoughby Ave	23.07	180	6.7	0.2455
R3	Northridge, 1994	Lake Hughes #4B - Camp Mend	31.69	90	6.7	0.0629
R4	Cape Mendocino, 1992	Fortuna – Fortuna Blvd	19.95	0	7.1	0.1161
R5	Northridge, 1994	Big Tujunga, Angeles Nat F	19.74	352	6.7	0.2451
R6	Landers, 1992	Barstow	34.86	90	7.4	0.1352
R7	San Fernando, 1971	Pasadena – CIT Athenaeum	25.47	90	6.6	0.1103
R8	Hector Mine, 1999	Hector	11.66	90	7.1	0.3368
R9	Kobe, 1995	Nishi-Akashi	8.70	0	6.9	0.5093
R10	Kocaeli (Turkey), 1999	Arcelik	53.7	0	7.5	0.2188
R11	Chi Chi(Taiwan), 1999	TCU045	77.5	90	7.6	0.5120
R12	Friuli(Italy), 1976	Tolmezzo	15.82	0	6.5	0.4169

[a]Closest Distance to Fault Rupture

Resistant Design of Buildings (Standard No. 2800 2014).In this equation, *H* is frame height from the base.

$$T = 0.08(H)^{0.75} \qquad (2)$$

Based on the results, it is evident that the system has considerably higher elastic stiffness in comparison with the ordinary eccentric braced frames. Moreover, due to the noticeable difference between the empirical and analytical vibration periods, the proposed empirical relation by the Standard No. 2800 (2014) is not applicable so that utilizing them leads to wrong estimations about seismic demands.

Vibration trend in the coefficients of the effective translational mass shows that increasing frame height can cause increase of higher modes participation in the seismic response of the structure (Mortezaei and Ronagh 2013).

The values of the vibration period and the coefficients of effective translational mass participation for the first mode show that the assumption of the triangular distribution of lateral forces in the equivalent static method provides acceptable design results.

3.2 Pushover analysis

For performing the pushover analysis, the modal pattern is selected in lateral loads distribution. This pattern is consistent with the effective modes and the number of these modes is selected such that more than 90 percent of frame mass participate in analysis (Table 2). In this study, the target displacement is derived from time history analysis by averaging the maximum roof displacements under artificial accelerograms (Table 3).

To use more compatible ground motions in the analysis, artificial accelerograms which are compatible with the design spectrum are used. Accordingly, 12 artificial accelerograms are developed based on the selected records (Table 4) by means of wavelet spectral matching method (Hancock *et al.* 2006). These artificial accelerograms are produced for demand spectra of the site according to the Iranian Code of Practice for Seismic Resistant Design of Buildings (Standard No. 2800 2014) considering type II soil and the first hazard level (return period of 475 years) (Fig. 6). The maximum acceleration in these artificial accelerograms is close to that of design earthquake (0.35 g). The utilized ground motions to produce artificial accelerograms are listed in Table 4.

In the following, in addition to evaluation of damage levels in the studied frames under the push-over loading, roof drift (ratio of roof displacement to frame height) is recorded when yielding is occurred in the vertical link and story beams. The value of drifts and capacity curves of the frames are demonstrated in Fig. 7.

Push-over analysis shows that the first yielding occurs in the panels of vertical links. According to the Fig. 8, increase in the height of structure would reduce its lateral stiffness. As the braces do not buckle, a sudden decrease does not exist in the lateral stiffness and strength of curves. It is obvious that the vertical links experience damage and dissipate energy before any other structural elements. These findings confirm that this system improves seismic behavior of frame structures under the design hazard level.

As can be seen in Fig. 8, axial strains in the brace are lower than the tensile and compressive limit strains in the immediate occupancy performance level. Therefore, all the braces remain in the mentioned performance levels both in compression and tension.

The story beams in the braced spans demonstrate the same performance. Based on the limit states of the vertical links (Fig. 5), the available stresses show acceptable accuracy of the system.

3.3 Incremental dynamic analysis

Lack of information about ground motions with different intensity and compatible with the site characteristics is a major challenge in seismic performance evaluation of structures. To overcome this difficulty, researcher applied constant coefficient to the available records which outcome is Incremental Dynamic Analysis (IDA). In this method, the concept of scaling ground motions is used to develop a new method for estimating seismic demand and capacity of structures in a wide range of elastic behavior to collapse (Vamvatsikos and Cornell 2002). In order to study the effects of variation in amplitude, frequency content and time duration of ground
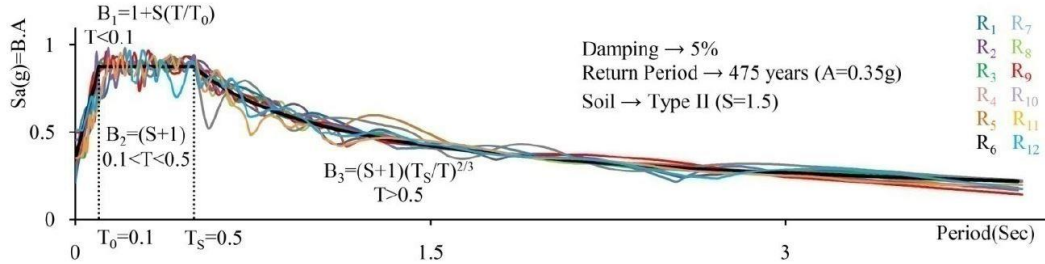
Fig. 6 Comparison of artificial accelerograms (R_i) spectra with the site demand spectrum
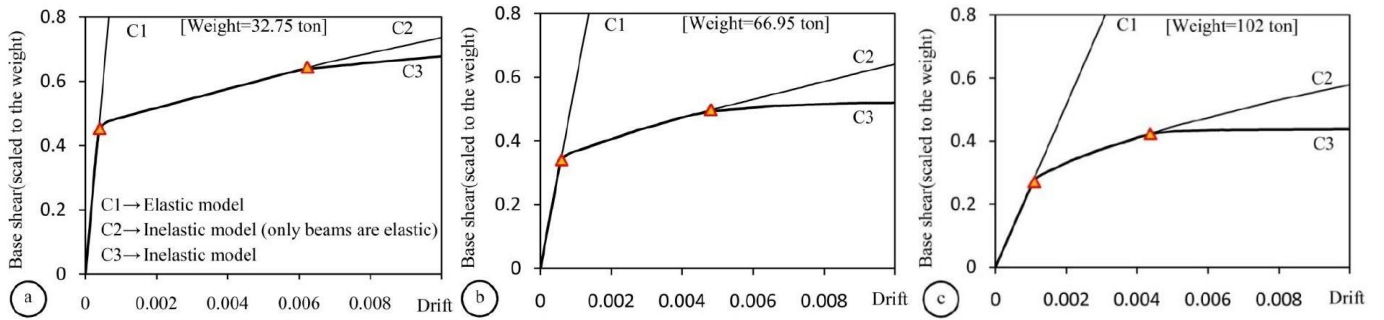

Fig. 7 Capacity curves of the frames and drift corresponding to the initiation of nonlinear behavior in vertical links and story beams (a) 4-story frame (b) 8-story frame (c) 12-story frame

motions on the structural response, IDA is also done considering the probable ground motions. Selection of the accelerograms and suitable parameters for intensity and seismic response are prerequisites of this study.

3.3.1 Selection of accelerograms

The first step in IDA is selecting consistent accelerograms with the site conditions. The utilized accelerograms must be able to reflect properties of the ground motions source, fault mechanism, distance from the fault, intensity and soil properties the site. In addition to the characteristics of records, number of the utilized accelerograms is also important. Using more accelerograms would reduce uncertainty in the analysis. According to the literature review, usually 10 to 20 ground motion records provide acceptable accuracy in the estimation of seismic demand in incremental dynamic analysis (Shome and Cornell 1999). Therefore, in this study 12 pair of far-fault ground motion records from the PEER (http://peer.berkeley.edu/smcat) database is used for IDA. The soil type of these ground motions is consistent with the site (type C of NEHRP classification, (360 m/s$\leq V_s \leq$760 m/s)). After developing the response spectrum for each pair of accelerograms, main component of the earthquake is selected based on the greater spectral values in the range of the structural periods.

3.3.2 Selection of the intensity and seismic response parameters

Intensity of the ground motions which increases during the analysis is demonstrated by intensity measure (IM) and the output of the analysis due to the applied excitation is designated by damage measure (DM). The IDA curves are in fact graphical representation of variation of the DM with respect to the IM.
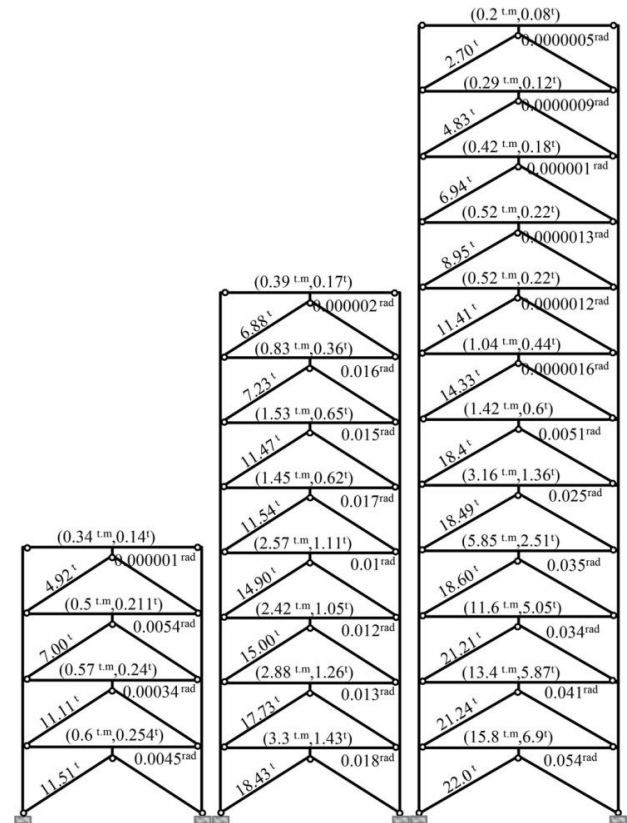

Fig. 8 Axial force of braces, shear and bending moment of the beams and shear strain of the links in the braced span

In this study, the maximum ground acceleration (PGA(g)) are selected as IM and the maximum shear deformations of the vertical links in each story are choosed as DM. Fig. 9 demonstrate developed curves from IDA with limit states of the vertical links (Fig. 5).
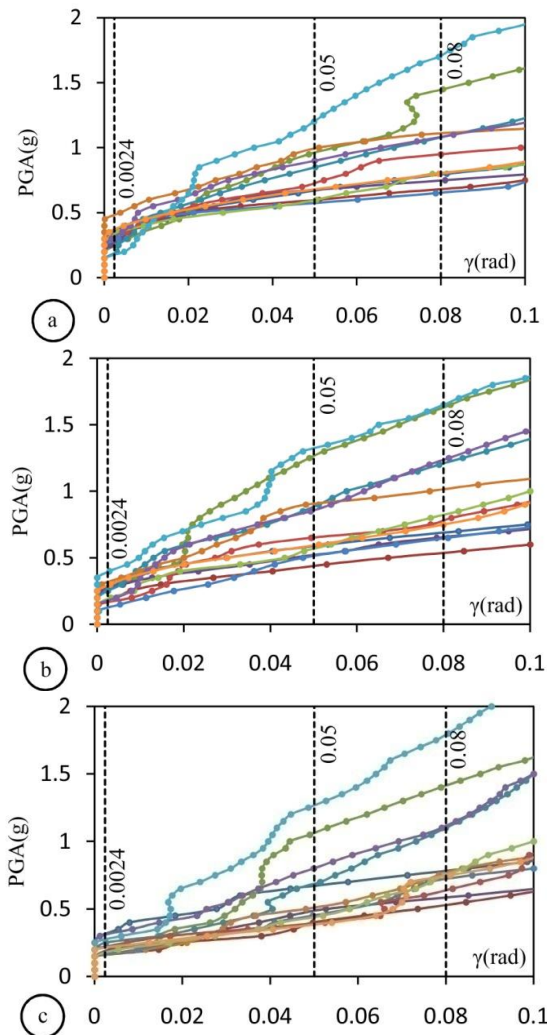
Fig. 9 Developed IDA curves and the limit states (a) 4-story (b) 8-story and (c) 12-story frame

Table 5 Average of maximum ground accelerations to cause different limit states in the vertical links(g)

	4 story frame	8 story frame	12 story frame
γ=0.0025 (rad)	0.30	0.24	0.22
γ=0.05 (rad)	0.78	0.76	0.63
γ=0.08 (rad)	0.98	0.96	0.91

Based on the results, shown in Table 5, it is evident that the average maximum acceleration which is necessary to cause higher performance levels in the vertical links is much higher than the intensity of maximum acceleration of design earthquake (0.35 g). Moreover, in these intensities, stress in the vertical links reaches the yield limit. This is more evident in the higher frames.

Evaluating the seismic dissipated energy of different elements in each story (beams, columns and braces) under the different intensity levels verify the fuse role of shear panels. For example, according to the Figs. 10 and 11, under the records with the maximum accelerations of 0.35 g and 0.55 g, the total seismic energy applied to the frame is dissipated by the vertical links in different stories (L_i). In this condition, it is obvious that the other structural
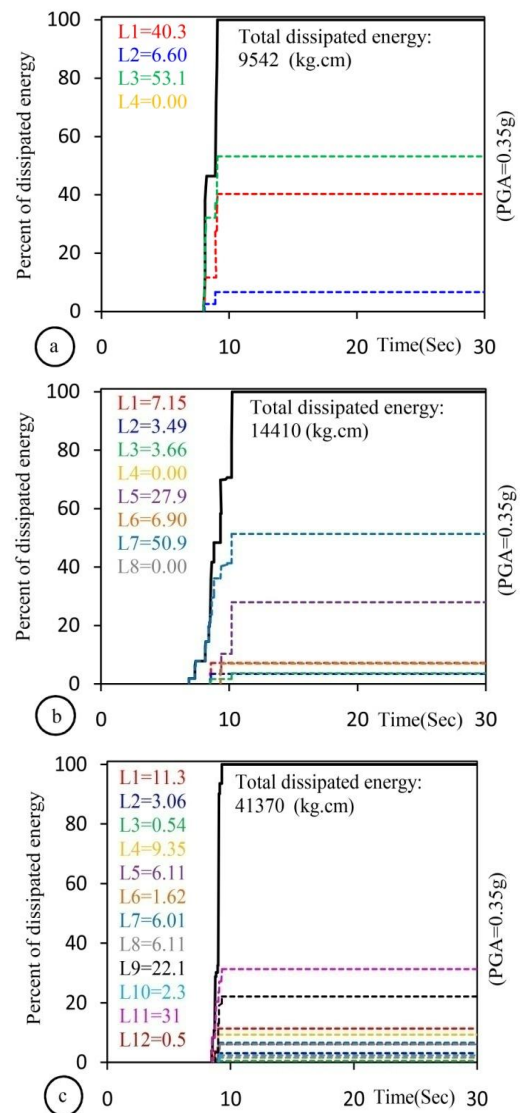

Fig. 10 Seismic dissipated energy of vertical links in each story (L_i) under the PGA=0.35 g (a) 4-story, (b) 8- story, and (c) 12-story frame

members remain in the elastic behavior range.

4. Seismic reliability analysis

There is a main question in the seismic reliability analysis: "In a certain location, which performance level occurs in the structure subjected to a given earthquake?".Answer this question faces many uncertainties. These uncertainties fall into two categories. The main group is natural uncertainties such as prediction of the future earthquakes, difference between the predicted and existing material properties and the environmental effects and so on. The other group is uncertainties due to errors in the modeling or computational methods and so on (Ang and Tang 2007; Berahman and Behnamfar 2007,). Because of this uncertain nature, the most logical method to answer this question is probability approach (Mortezaei, 2014).
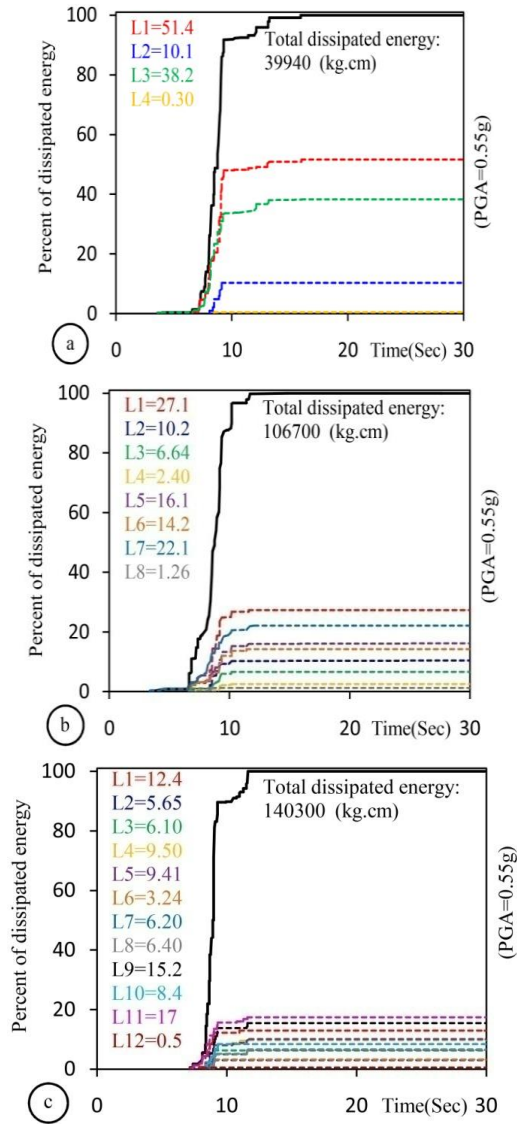
Fig. 11 Seismic dissipated energy of vertical links in each story (L_i) under the PGA=0.55 g (a) 4-story, (b) 8-story, and (c) 12-story frame

It is possible to determine a certain performance level under the different earthquake intensities (IM-Based), instead of intensity level determination which produces different performance levels. In another way, for a given hazard level, it is possible to compute the likelihood that the structural response reaches a limit state corresponding to various damage levels (EDP-Based) (Zareian *et al.* 2010).

4.1 Failure of the structure based on the seismic intensity (IM-Based)

In this approach, the seismic intensity is analysis variable that determines the damage limit states in the structure. The probability to reach an assumed limit state ($P(f)$) can be computed from the Eq. (3).

$$P(f) = P[C \mid IM = im_i] = P[im_i > IM_C]$$
$$= 1 - F_{IM_C}(im_i) \tag{3}$$

Where, $F_{IM_C}(im_i)$ is the cumulative probability function of the seismic capacity. It is obvious that when all of the input parameters and the earthquake effects are deterministic, this function is equal to one or zero. The fact is that existence of uncertainties may change capacity parameters of the structure. In Eq. (3), I_{Mc} and $P[C \mid IM=im_i]$ are the critical limit state of seismic intensity and the cumulative probability of failure for a give intensity (im_i), respectively.

4.2 Failure of the structure based on the earthquake demand parameter (EDP-Based)

In this approach, the engineering demand parameter is a critical variable that determines the failure limit state in the structure. Eq. (4) is the mathematical representation of this limit state.

$$P(f) = P[C \mid IM = im_i] = P[EDP_d > EDP_c \mid IM = im_i]$$
$$= \sum_{all(edp_C)} P[EDP_d > EDP_c \mid EDP_c = edp_{ci}, IM = im_i] \tag{4}$$
$$\times P[EDP_C = edp_{ci}]$$

In this equation, EDP_d and EDP_c are the engineering demand parameters for demand and capacity, respectively, and, dep_c is the response corresponds to a given failure level. For a given EDP_c, it is possible to compute $P[EDP_d>EDP_c|EDP_c=edp_{ci}]$ (the probability that engineering demand parameter exceeds the capacity if engineering capacity parameters reaches a certain level, i), and $P[EDP_d>EDP_c|EDP_c=edp_{ci}]$ (the probability that engineering capacity parameter reaches a certain level, i) for each im_i. Then by summation of these probabilities for all of the edp_c in each intensity measure (im_i), the failure probability, $P(f)$, will be computed.

In the present study, the fragility curves are derived for different performance levels. Hence, for different seismic intensities, the probability that vertical link deformation reach limit values corresponding to different failure levels are determined. For the studied frames, the maximum shear deformation of vertical links (γ) is selected as the response. The limit states of the strains which are depicted in Fig. 5, are considered as failure criteria in the frames. Quantitative values, shown in the Fig. 5, are related to these limit states, i.e., 0.0024, 0.05 and 0.08. The procedure goes through following steps:

The maximum ground accelerations are derived from the IDA curves. It is assumed that these values have lognormal distribution. After computing the mean (μ) and the standard deviation (δ) for the derived values, the probability density function (F(X)) is determined. As depicted in Fig. 12, for a given $X0$ as an intensity level, the area under the curve from $-\infty$ to $X0$ represent the probability of exceedance of intended performance level (P) at the given intensity (Mohsenian *et al.* 2016). The fragility curves for a given failure level are developed by using this approach for all of the frames considering different earthquake intensities. Developed curves for the studied frames are depicted in Fig. 13.

Based on these curves and the quantitative values presented din Tables 6, for both design and maximum
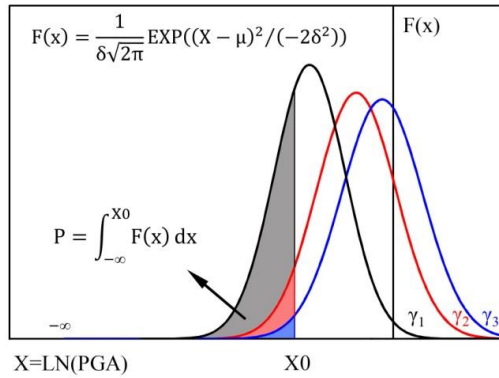
Fig. 12 Probability of exceedance of constant limit states $\gamma 1$, $\gamma 2$ and $\gamma 3$ for a hazard level like $X0$ (Schematic)

Table 6 Probability of exceedance of different failure levels under the design and maximum probable earthquakes

Models →	4 story frame		8 story frame		12 story frame	
PGA→	0.35 g	0.55 g	0.35 g	0.55 g	0.35 g	0.55 g
γ=0.0024 (rad)	73.6	98.8	89.8	99.7	97.7	99.9
γ=0.05 (rad)	0	7.8	2.4	23.4	10.6	44.9
γ=0.08 (rad)	0	3.3	0.6	9.1	0.7	11.4

two parameters increases probability of exceedance of the limit states corresponding to different performance and failure levels.

5. Multi level evaluation of the response reduction factor

There are three different types of response reduction factor according to the literature and technical terminology, namely design (force or code) factor, demand (displacement or ductility) factor and supply (capacity) response reduction factor (Beheshti-Aval 2013). To prevent any misunderstanding, these concepts will be defined clearly in the following.

5.1 Design (Code) response reduction factor (R_{Code})

The proposed values of response reduction factor for different structural systems by the seismic codes are based on the observed seismic performance of the systems in the previous ground motions and are somehow on the engineering justifications. Some researchers have been done studies to prove that these code factors are not reliable and believe that estimation of more accurate responses would increase reliability of the design code requirements (Bertro 1989). The main reason to entitle these type of response reduction factors as "force method" factors is that the ductility demand is not included in their evaluation. In Iranian Code of Practice for Seismic Resistant Design of Buildings (Standard No. 2800 2014), R_{Code} values are suggested only according to the structural system and material, without considering the structural period of vibration. In the present study, the utilized response reduction factor for preliminary design of the frames was 7 according to the Standard No. 2800 (2014) for special eccentric braced frames.

5.2 Demand (Displacement/Ductility) response reduction factor (R_{Demand})

This factor depends on the seismic hazard level and physical and geometrical properties of the structure. Previous studies show that intensity and focal depth of the earthquake don't have considerable effects on R_{Demand} factor and parameters such as ductility, energy dissipation capacity, vibrational period of the structure, over-strength, redundancy, degrees of freedom and soil type of the site are more effective (ATC 1995a, Miranda 1991, Lia and Biggs 1980). The demand response reduction factor in this study is derived directly for the multi-degrees-of-freedom system
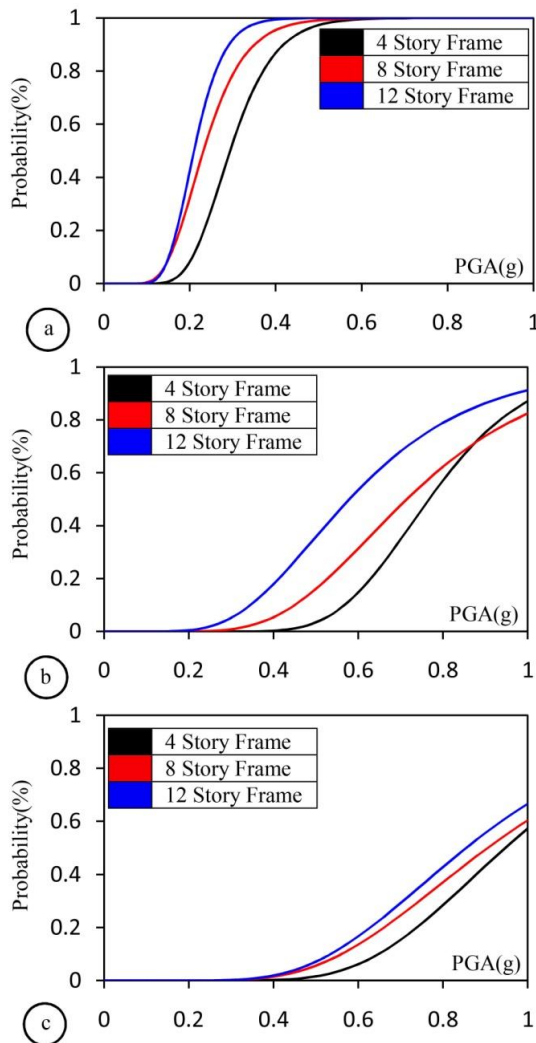

Fig. 13 Fragility curves for different limit states in the vertical links (a) γ=0.0024 rad (b) γ=0.05 rad (c) γ=0.08 rad

probable hazard levels, the vertical links reaches shear yielding, but the system has high reliability for the higher damage levels.

It is obvious that the system has acceptable ability to dissipate energy of possible aftershocks in severe ground motions. As can be seen, the system response is sensitive to the applied excitation and frame height. Increase in these
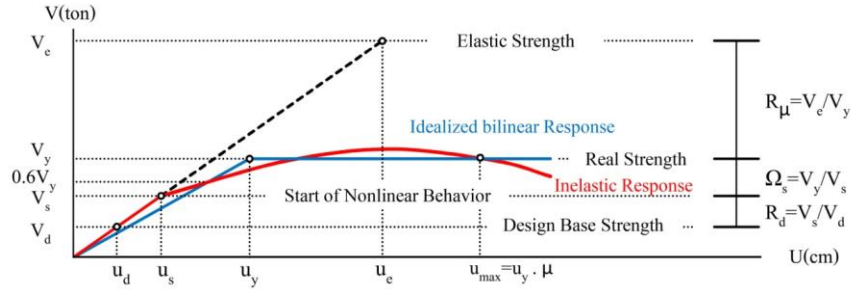
Fig. 14 Idealization of the structures' capacity curve and introduction of the parameters used for calculation of the response modification factor (FEMA 356 2000)

Table 7 Response reduction factors of demand and capacity in the studied frames

Shear values are reported in (Ton)	4 story frame		8 story frame		12 story frame	
	R_{Demand}	R_{Supply}	R_{Demand}	R_{Supply}	R_{Demand}	R_{Supply}
Average of the PGA (g)	0.35	0.855	0.35	0.74	0.35	0.69
Elastic strength (V_e)	25.5	71.12	45.85	147.73	58.47	195.6
Real strength (V_y)	14.7	15.37	24.40	26.26	29.08	30.86
strength for the start of nonlinear behaviors (V_s)	14.52	14.52	23.53	23.53	27.55	27.55
Design base strength (V_d)	8.20	8.20	16.74	16.74	21.5	21.5
Response modification factor due to ductility (R_μ)	1.735	4.63	1.88	5.63	2.01	6.34
Response modification factor due to over strength (Ω_s)	1.012	1.06	1.037	1.116	1.055	1.12
Response modification factor due to allowable stress (R_d)	1.77	1.77	1.40	1.40	1.28	1.28
Response modification factor ($R_\mu=R_\mu.\Omega_s.R_d$)	3.11	8.67	2.74	8.82	2.72	9.1

by using the following equation

$$R_{Demand} = R_\mu^{MDOF}.\Omega_S.R_d \qquad (5)$$

Where R_μ^{MDOF} is the response reduction factor due to ductility and dissipated energy by hysteresis behavior, Ω_S is over-strength factor of the structure that implicitly account for redistribution of forces as a results of the redundancy. R_d is called reduction factor in allowable stress design and includes the effects of reduced strength which is necessary in the allowable stress or strength design method. In the following the necessary steps to derive these factors is described:

For a given hazard level, demand spectrum is derived and the accelerograms which are compatible with this spectrum are selected. Assuming linear behavior, the selected accelerograms which are called demand ground motions are applied to the structure, and the resulted base shears are recorded. Average of these values is called elastic base shear (V_e). In this study, as the objective hazard level is design earthquake, to provide more compatibility with the site condition, the artificial accelerograms discussed in section 4.2, are used.

In the next step, demand earthquakes are applied to the structure, but in this step nonlinear behavior is considered. The maximum roof drifts resulted from the analyses are recorded. Average of these values is taken as the target displacement of the design earthquake (Table 3) on the capacity curve derived from pushover analysis. After bi-linearization of the capacity curve according to the guidelines, real strength, (V_y), is computed (FEMA 356 2000).

The base shear corresponding to the initiation of nonlinear behavior (V_s), is the point where linear capacity curve disparts from the nonlinear one, according to the Fig. 13. Design base shear (V_d) is derived from dividing the multiplication of spectrum acceleration obtained from linear spectrum by the overall weight on the code reduction factor (($S_a.W$)/R_{code}). Finally, the necessary parameters for calculating the demand response modification factor are computed by using Eq. (5) and the relationships depicted in Fig. 14. These parameters for computing the demand response reduction factor of frame structure with slender braces and the frame equipped with the dampers are listed in Table 7.

5.3 Supply (capacity) response reduction factor (R_{Supply})

This factor depends on the capacity of the structure in the nonlinear deformations and defined performance levels. Design of the structures can be done like before using the force method and selecting the strength reduction factor based on the assumption of a specific damage level under the design earthquake. This performance based idea is used currently to evaluate seismic vulnerability of the existing structures (Fajfar 2000). The utilized algorithm for derivation of the supply response reduction factor according to ATC (1996) and based on the lateral strength is as follows:

Incremental dynamic analysis is done using the site accelerograms and including the nonlinear behaviors. PGA factors of target damage level are recorded which in this study are the drifts corresponding to the maximum strength and the first buckling of the diagonal braces. Then, linear
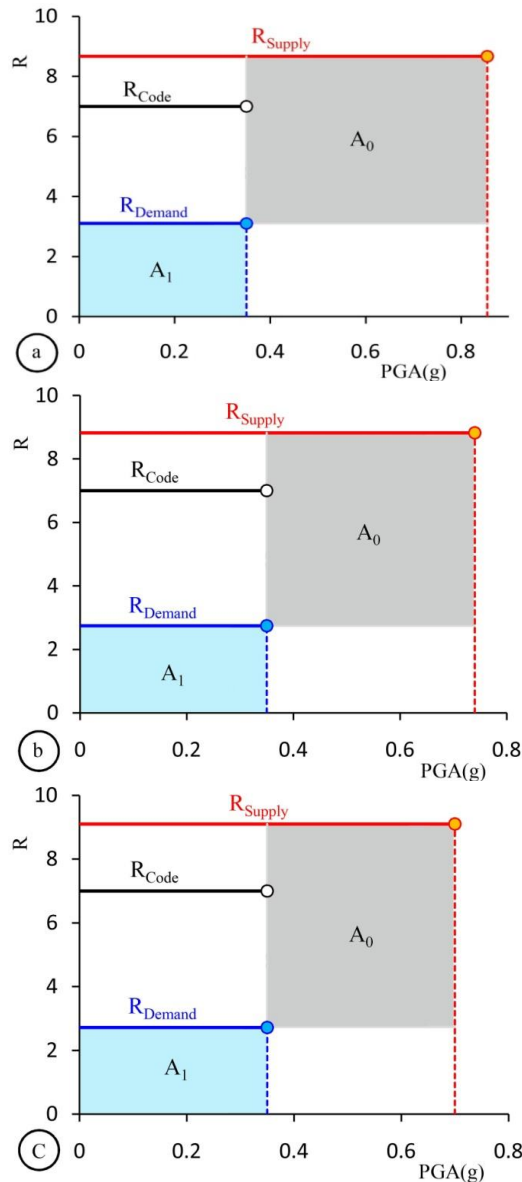
Fig. 15 Comparison of the demand, supply and code response reduction factors of (a) 4-story frame (b) 8-story frame (c) 12-story frame

dynamic analysis is achieved under the recorded PGA from the previous step and average of the derived base shears, (V_e), is computed. In additional step, pushover analysis is performed using the modal lateral load pattern and the capacity curve of frame is derived. The capacity curve is bi-linearized by taking the target displacement of the considered damage levels in the first step and the equivalent yield shear of the frame, (V_y), is derived from this idealized curve. The next steps are same as those for computation of the demand response reduction factor. The derived values are listed in Table 7 for both structures with and without dampers.

It is evident that the supply response reduction factor of the rehabilitated frame and its hazard level is higher than the demand response reduction factor and the design hazard level. This confirms high strength and enough safety of the proposed system for extreme hazard level (Fig. 15).

In the frames, for each pair in the A_1 area, system remains in the elastic range. Therefore, when the design earthquake and the response reduction factor of 3 (Standard No. 2800 2014) are used by the designer, the system would remain in the elastic range. It is obvious that selection of the demand response reduction factor between the demand and capacity values for a given damage level would guarantee the fact that the frame performs in the desired performance level for this hazard level. For example, for each pair of the values in the gray area (A_0), the frame still has ability to sustain lateral load. As can be seen in Fig. 15, selecting the code response reduction factor of 7 for preliminary design of the structure completely guaranty safety and energy absorption capacity of the lateral load bearing elements under the design earthquake, and deformations of the vertical links remains in allowable code limits (Table 5). Consequently, the results show that the code factor of 7 is always in the safe region. According to the Fig. 15, for the design earthquake and lower intensities, the maximum response modification factor of 8.5 will be safe. The parametric study shows that increase in the height would increase the ductility (R_μ) and over strength (Ω_s) factors in the demand and capacity response reduction factors. This is more evident in the case of ductility factor.

6. Conclusions

The results show that due to design flexibility, effectiveness and practicality advantages, eccentric braced frames with vertical links are useful and efficient systems for rehabilitation of the existing structures. Because of the many advantages, this system can be considered as independent lateral load bearing capacity in the seismic design codes. The main results of this study are concluded as bellow:

• Assumption of triangular distribution of the lateral earthquake forces for analysis and design of eccentric braced frames with vertical connections is an appropriate notion.

• Available empirical relationship in the design codes for evaluation of vibrational period of the similar lateral load bearing systems cannot provide acceptable estimates for the studied system.

• The vertical links has high energy dissipation capacity. They absorb and dissipate all of the applied seismic energy. Therefore, the assumption that other frame elements remain elastic is correct.

• No sudden drop in the strength and stiffness is evident in capacity curve of the frame. After yielding of the links in each story, lateral load remains constant, hence, the braces must be designed based on the shear capacity of the vertical links.

• Depending on the hazard and desired performance level, the system has acceptable seismic reliability and is easy to use.

• Under the design hazard level, the stress in the vertical links reach to the yield level and the axial strains in the brace elements are lower than the value corresponding to the immediate occupancy level. Moreover, the shear

force and bending moments of the story beams are also considerably lower than the corresponding capacities.

• Under the design hazard level (0.35 g), the probability of shear yielding in the vertical links for the 4, 8 and 12 story buildings are evaluated equal to 73.6, 89.8 and 97.7 percent, respectively. Under the maximum probable earthquake (0.55 g), the probability of exceedance of allowable axial strains in the links for all of the studied frames is reported to be less than 12 percent. This shows sufficient safety margin under severe earthquakes and the acceptable energy absorption capacity of the system even for high seismic intensities.

• The demand response reduction factors of the studied frames are slightly less than 3. This low value means that the system quickly experience nonlinear deformations due to shear yielding of the links under the design hazard level.

• The capacity response reduction factor and the corresponding intensity for the 4 story frame are equal to 8.67 and 0.85 g, respectively. For the 8 story frame these values are equal to 8.82 and 0.74 g and finally for the 12 story structure, they are reported as 9.1 and 0.69 g. It is evident that the corresponding intensities are remarkably higher than the design earthquake (0.35 g).

• Under the design hazard level, the code response reduction factor equal to 7 is less than the capacity factor and higher than the demand response modification factor. This proves that using the code factor for preliminary design of frames is suitable. Based on the findings, using response reduction factor equal to 8 also provide desirable outcomes.

• Increase in the height of the frame would increase both ductility and over strength response modification factors (R_μ, Ω_S). This increase is more evident in the case of ductility factor.

References

ABAQUS (2014), Version 6.14, ABAQUS Users Manual, SIMULIA World Headquarters, Rissing Sun Mills 166 Valley Street, Providence, RI 02909-2499, USA.

Ang, A.H.S and Tang, W.H. (2007), *Probability Concepts in Engineering: Emphasis on Applications to Civil and Environmental Engineering*, Vol. 1, Wiley, 2nd Edition, USA.

ATC (1995a), "Structural response modification factors", ATC-19 Report, Applied Technology Council, Redwood City, California.

ATC (1996), *Seismic Evaluation of Concrete Buildings*, Vol. 1, ATC-40, Applied Technology Council, Redwood, CA.

Baradaran, M.R., Hamzezarghani, F., Rastegari Ghiri, M. and Mirsanjari, Z. (2015), "The effect of vertical shear-link in improving the seismic performance of structures with eccentrically bracing systems", *Int. J. Civil Environ. Eng.*, **9**(8), 1078-1082.

Bathaei, A. and Zahrai, S.M. (2017), "Investigation of the effects of vertical link beam length on steel structures residual displacement", *Modares Civil Eng. J.*, **17**(3), 47-60. (in Persian)

Beheshti Aval, S.B. (2013), *Seismic Rehabilitation of Existing Buildings*, Vol. 1, K.N. Toosi University of Technology Press, Iran.

Berahman, F. and Behnamfar, F. (2007), "Seismic fragility curves for un-anchored on-grade steel storage tanks: Bayesian approach", *J. Earthq. Eng.*, **11**(2), 166-192.

Bertro, V.V (1989), "Evaluation of response reduction factors recommended by ATC and SEAOC", *Proceedings of the 3rd U.S.Natl Conf. on Earthquake Engineering*, South Carolina, 1663-1670.

Bouwkamp, J., Vetr, M.G. and Ghamari, A. (2016), "An analytical model for inelastic cyclic response of eccentrically braced frame with vertical shear link (V-EBF)", *Case Stud. Struct. Eng.*, **6**, 31-44.

Computers and Structures Inc. (CSI) (2015), Structural and Earthquake Engineering Software, ETABS, Extended Three Dimensional Analysis of Building Systems Nonlinear, Version 15.2.2, Berkeley, CA, USA.

Computers and Structures Inc. (CSI) (2016), Structural and Earthquake Engineering Software, PERFORM-3D Nonlinear Analysis and Performance Assessment for 3-D Structures, Version 6.0.0, Berkeley, CA, USA.

Daryan, A.S., Bahrampoor, H., Ziaei, M., Golafshar, A. and Assareh, M.A. (2008), "Seismic behavior of vertical shear links made of easy-going steel", *Am. J. Eng. Appl. Sci.*, **1**(4), 368-377.

Duan, L. and Su, M. (2017), "Seismic testing of high-strength steel eccentrically braced frames with a vertical link", *Proc. Inst. Civil Eng. Struct. Build.*, **170**(11), 874-882.

Fajfar, P. (2000), "A nonlinear analysis method for performance based seismic design", *Earthq. Spectra*, **116**(3), 573-592.

FEMA 356 (2000), Prestandard and Commentary for the Seismic Rehabilitation of Buildings, Prepared by the American Society of Civil Engineers for the Federal Emergency Management Agency, Washington D.C.

Hancock, J., Watson-Lamprey, J., Abrahamson, N.A., Bommer, J.J., Markatis, A., McCoy, E. and Mendis, R. (2006) "An improved method of matching response spectra of recorded earthquake ground motion using wavelets", *J. Earthq. Eng.*, **10**, 67-89.

Institute of National Building Regulations (2008), Design and construction of Steel Structures, Topic. 10, Ministry of Roads & Urban Development, Iran.

Lia, S.P. and Biggs, J.M. (1980), "Inelastic response spectra for seismic building design", *J. Struct. Div.*, ASCE, **106**(6), 1295-1310.

Lian, M. and Su, M. (2017), "Seismic performance of high-strength steel fabricated eccentrically braced frame with vertical shear link", *J. Constr. Steel Res.*, **137**, 262-285.

Miranda, E. (1991), "Seismic evaluation & upgrading of existing buildings", A P.hd Thesis, University of California @ Berkeley.

Mohsenian, V., Gharehbaghi, S.A. and Beheshti-Aval, S.B. (2016), "Seismic reliability assessment of two case-study tunnel form buildings considering the effect of soil-structure interaction," *Bull. Earthq. Sci. Eng.*, **3**(3), 11-29. (in Persian)

Mortezaei, A. (2013), "Plastic hinge length of RC columns considering soil-structure interaction", *Earthq. Struct.*, **5**(6), 679-702.

Mortezaei, A. and Ronagh, H.R. (2013), "Effectiveness of modified pushover analysis procedure for the estimation of seismic demands of buildings subjected to near-fault ground motions having fling step", *Nat. Hazard. Earth Syst. Sci.*, **13**(6), 1579-1593.

PEER Ground Motion Database, Pacific Earthquake Engineering Research Center, Web Site: http:// peer.berkeley.edu/peer-ground-motion-database

Permanent Committee for Revising the Standard 2800 (2014), Iranian Code of Practice for Seismic Resistant Design of Buildings, 4th Edition, Building and Housing Research Center, Tehran, Iran.

Rahnavard, R., Hassanipour, A., Suleiman, M. and Mokhtati, A. (2017), "Evaluation on eccentrically braced frame with single and double shear panels", *J. Build. Eng.*, **10**, 13-25.

Seki, M., Katsumata, H., Uchida, H. and Takeda, T. (1988), "Study on earthquake response of two-storied steel frame with Y-shaped braces", *Proceedings 9ᵗʰ World Conference on Earthquake Engineering*, Tokyo-Kyoto, Japan.

Shayanfar, M.A., Barkhordari, M.A. and Rezaeian, A.R. (2011), "Experimental study of cyclic behavior of composite vertical link in eccentrically braced frames", *Steel Compos. Struct.*, **12**(1), 13-29.

Shome, N. and Cornell, C.A. (1999), "Probabilistic seismic demand analysis of nonlinear structures", Reliability of Marine Structures Report No: RMS-35, Civil and Environmental Engineering, Stanford University.

Vamvatsikos, D. and Cornell, C.A. (2002), "Incremental dynamic analysis", *Earthq. Eng. Struct. Dyn.*, **31**(3), 491-514.

Vetr, M.G., Ghamari, A. and Bouwkamp, J. (2017), "Investigating the nonlinear behavior of eccentrically braced frame with vertical shear links (V-EBF)", *J. Build. Eng.*, **10**, 47-59.

Zahrai, S.M. and Mahroozadeh, Y. (2010), "Experimental study of using vertical link beam to improve seismic performance of steel buildings", *J. Civil Surv. Eng.*, **44**(3), 379-393.

Zahrai, S.M. and Moslehi Tabar, A. (2013), "Analytical study on cyclic behavior of chevron braced frames with shear panel system considering post-yield deformation", *Can. J. Civil Eng.*, **40**(7), 633-643.

Zahrai, S.M. and Parsa, A. (2015), "Effect of flange width of vertical link beam on cyclic behavior of chevron braced steel frames", *J. Seismol. Earthq. Eng.*, **17**(4), 281-292.

Zareian, F., Krawinkler, H., Ibarra, L. and Lignos, D. (2010), "Basic concepts and performance measures in prediction of collapse of buildings under earthquake ground motions", *Struct. Des. Tall Spec. Build.*, **19**, 167-181.

AT